

SDSS-IV DR17 Looking at the Radial Relationships between Dust Attenuation and Dust Kinematics

DANIEL KRISTA-KELSEY¹

¹*University of Massachusetts - Amherst
710 N Pleasant St
Amherst, MA 01003, USA*

ABSTRACT

SDSS-IV has come out with a brilliant database of surveyed galaxies with their newly released and final addition, Data Release 17. We utilized their survey and Marvin, a Python package, to explore the radial correlations of galaxy properties and characteristics by taking advantage of MaNGA, a component that maps out many different locations of a singular galaxy, for all galaxies surveyed. We present an in-depth analysis of dust attenuation, derived from the Balmer decrement, where measurements were taken from the SED of each spaxel in the galaxy map of Plate ID = 8131-9101. By comparing the derived attenuation map with maps of star-forming spaxel regions and galaxy kinematics, a deeper understanding of the effects of attenuation can be understood.

Keywords: SDSS — Marvin — attenuation — galaxies — MaNGA

1. INTRODUCTION

As amazing as galaxies are, with the light of their stars brightening up the dark Universe, they also serve as excellent tools for humankind to explore the unknown. Simply put, galaxies are giant clusters of stars, gas, and dust glued together by gravity. One may ask, if galaxies exist, then how did they form and where did they come from and how did they form? Astronomers have been tackling this question for centuries now by taking advantage of the laws and physics of the Universe, and manipulating light to obtain vital information about galaxy formation history. Collecting information such as the spectral energy density (SED), kinematics, color, and its geometrical appearance has allowed scientists to extrapolate the Universe’s history and discover new fundamental principles the Universe abides by.

In order to explore this realm, astronomers construct and use ground-based and space telescopes to gather the light from these distant galaxies. From this, we can calculate how many stars a galaxy creates, how far away a galaxy is, and create a picture of what the galaxy looks like. Telescopes aren’t perfect though; local and distant factors affect the quality of observations, where some examples of said factors are atmospheric noise and absorption, dust obscuration, doppler effects, and gravitational lensing. These obstacles have garnered scientists all over the world to create instruments to best overcome the quality-disrupting variables and do research on the

resulting data to produce even more amazing results, which is where MaNGA comes in.

MaNGA, an abbreviation for Mapping Nearby Galaxies at APO (Apache Point Observatory), is one of the components of the Fourth Generation Sloan Digital Sky Survey (SDSS-IV). As of its Data Release 17, the survey has completed its goal of collecting kinematic and compositional data for a complete sample of around 10,000 galaxies using integral field unit (IFU) spectroscopy. Thus data can be used to explore each galaxy’s emission line fluxes, and gas and stellar kinematics, along with stellar population properties. For even more of an in-depth study of a singular galaxy, their radial property changes can be observed to see how characteristics of a galaxy can change in different locations, including structure, spectral features, density, velocity, and more. One thing that this paper emphasizes on is that MaNGA has collected very precise SEDs over an array of IFUs that maps out different parts of a singular galaxy, allowing a deeper exploration potential into the radial characteristic correlations. More specifically, we are interested in how attenuation maps out in the spacial dimensions of a galaxy and exploring a potential pattern in gas kinematics. In Section 2, we discuss the target galaxy in question to explore and its characteristics of itself and within the population. In Section 3, we explain how we utilize Marvin (explained in Section 2) to observe the galaxy and show our calculations. In Section 4, we discuss the results and impact, and analyze the results.

2. TARGET SELECTION AND METHOD

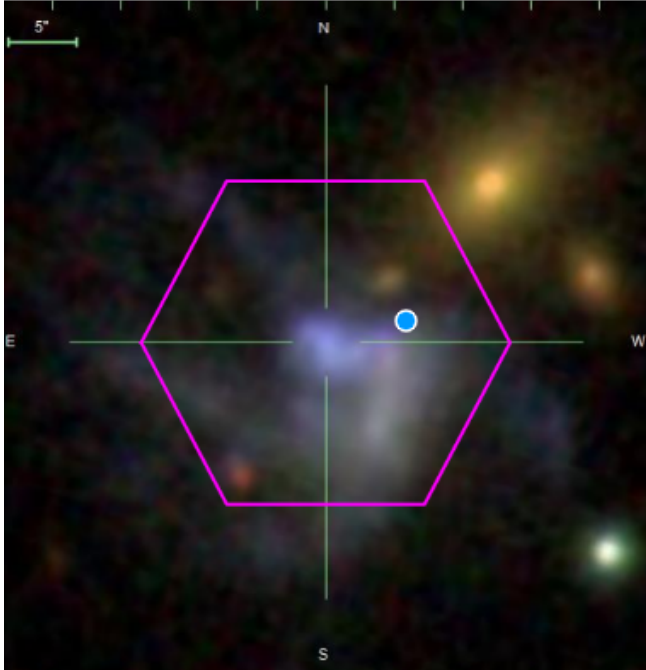


Figure 1. Image of 8131-9101. Resembles a young, blue barred spiral galaxy. The magenta hexagon around the galaxy is the IFU field.

2.1. *Marvin*

Marvin is a toolkit that is composed of a web interface, an Application Programming Interface, and, most importantly for this paper, a Python package, as discussed by [Cherinka et al. \(2019\)](#). For the purposes of SDSS-IV, Marvin allows one to either virtually access a database of galaxies surveyed by MaNGA, or to install information locally and use its Python package to unravel the data. Key highlights of modules within the package include ‘datacubes’ of galaxies, which contain spacial and wavelength information for each spaxel of the observed galaxy, and ‘maps’ of the galaxy that holds characteristic quantities for each spaxel.

2.2. *Selection*

Through the use of Marvin’s web interface, we randomly selected a galaxy with the Plate ID = 8131-9101, or MaNGA ID = 1-604748 (refer to Figure 1). The magenta hexagon is the IFU field, of which the spaxels cover. Since it is a young, blue barred spiral-like galaxy, there is an inferred large amount of star forming activity and there is likely to be a lot of gas and dust. This is a prime galaxy selection to observe radial dust attenuation. Likewise, we will also be looking at the gas and

Table 1. Galaxy Properties

Type	Value
z	0.05
$\log M_{\odot}$	9.871
Sérsic n	3.054
M	-21.0988
$g-r$	0.216
R-band half radius	7.992"
RA	112.574
DEC	39.942

NOTE—Galaxy Properties.
Note: Missing SFR, was not listed in Marvin - have to calculate manually via SED.

dust kinematics to observe if there is any correlation with attenuation.

2.3. *Galaxy Properties*

Refer to Table 1 for the galaxy characteristics. In terms of how this galaxy’s properties stand in comparison to the complete sample of 100,000 galaxies, it belongs to the upper-third quartile of the sample, it is a little less massive than the median galaxy mass, it has higher than average central concentration, it is brighter than the average galaxy, and it’s half-light radius is much higher than the average galaxy.

3. ANALYSIS

3.1. *Attenuation Calculation*

Before the analysis of the galaxy, we have to understand the calculation for attenuation. Attenuation is the extinction of dust, where gas and dust block the path of light, but attenuation also accounts for the geometry that recombines other sources of light back into the path of light. The most important measurement from the galaxy that was obtained using Marvin was the Balmer decrement, calculated from taking the ratio of $H\alpha/H\beta$. [Groves et al. \(2011\)](#) states that this ratio is a form of measurement of the reddening due to dust absorption. The intrinsic ratio of unattenuated SED $H\alpha$ and $H\beta$ lines is 2.87, and any deviation from this number is due to attenuation ([Domínguez et al. \(2013\)](#)). Using the Balmer decrement, we can calculate the color excess $E(B - V)$:

$$E(B - V) = 1.97 \log_{10} \left[\frac{(H\alpha/H\beta)_{\text{obs}}}{2.87} \right] \quad (1)$$

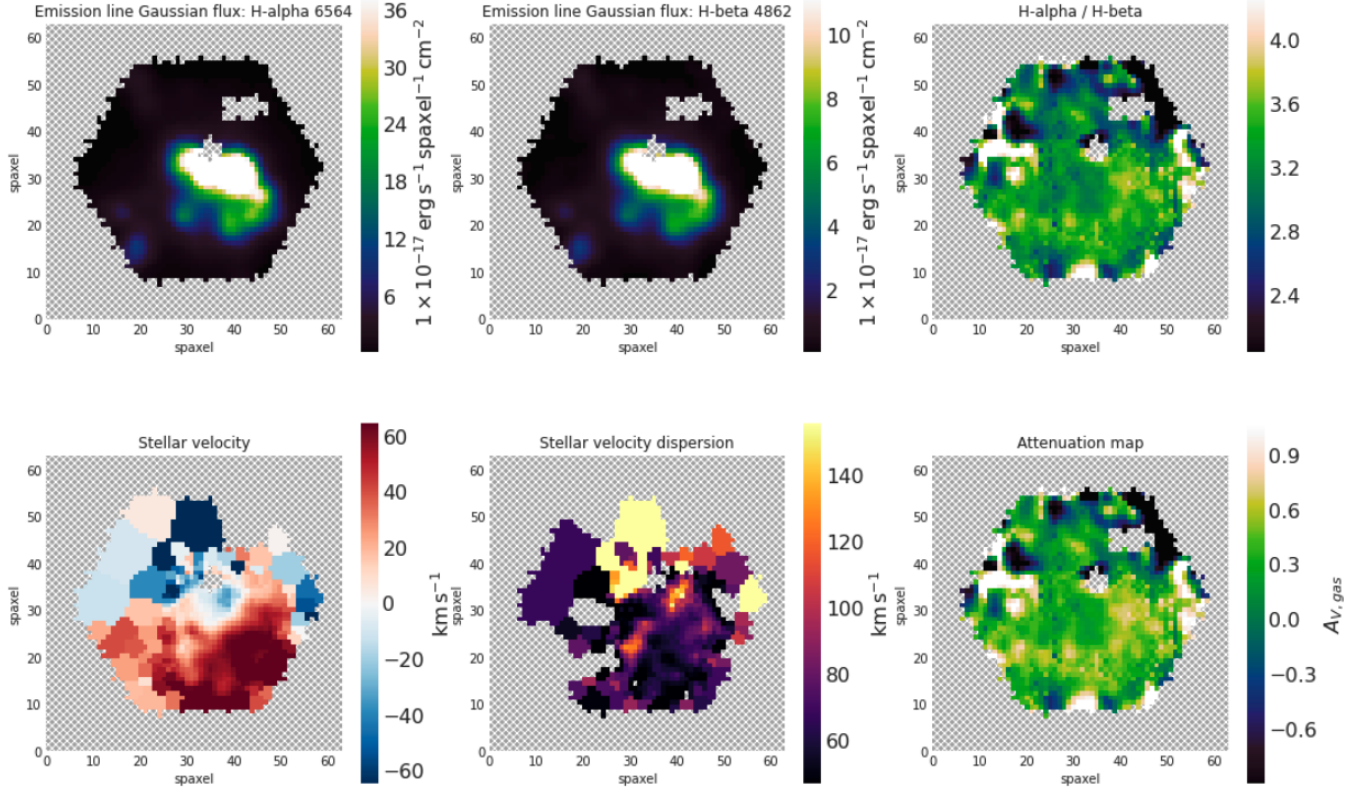


Figure 2. Top left: $\text{H}\alpha$ emission fluxes. Top middle: $\text{H}\beta$ emission fluxes. Top right: Balmer decrement, $\text{H}\alpha/\text{H}\beta$ ratio. Bottom left: Stellar velocity map. Bottom middle: Stellar velocity dispersion. Bottom right: Map of each spaxel’s dust attenuation, as calculated from Equation (2).

Equation (1) assumes an electron temperature of $T_e = 10^4 \text{ K}$ and the intrinsic $\text{H}\alpha/\text{H}\beta$ value (Greener et al. (2020)). If R_λ is the ratio of dust attenuation at wavelength λ , A_λ , and $R_V = 3.1$ for attenuation in the gas from the Balmer decrement, the attenuation can be determined:

$$A_V = 3.1E(B - V) \quad (2)$$

and the attenuation can be calculated for every spaxel in the galaxy.

3.2. Methods

In order to figure out the Balmer decrement, we obtained spacial maps of the $\text{H}\alpha$ and $\text{H}\beta$ emissions as shown in Figure 2. Using Marvin’s special tool, EnhancedMap, we can do arithmetic with these maps to produce a maps of the Balmer decrement, shown in Figure 2 as well. Using this ratio in Equation (1), and then in Equation (2), produces the dust attenuation map in the visible spectrum, $\lambda = 5500\text{\AA}$, for A_V , given $R_V = 3.1$. In Figure 2 and Figure 3, we present the maps of stellar velocity and dispersion, and gas velocities for $\text{H}\alpha$ and $\text{H}\beta$. We have also included a BPT diagram (Baldwin, Phillip, & Terlevich), where a description of a BPT diagram can be found in Kewley et al. (2006).

4. RESULTS AND DISCUSSION

4.1. Results

We can immediately see that, alone in the attenuation map, that most of the dust attenuation occurs on the outskirts of the IFU sensors. If compared to the star forming region derived from Figure 5, most of the obscuration occurs in the non-star-forming regions. This stands true as well for the emission line fluxes of $\text{H}\alpha$ and $\text{H}\beta$. When looking at the stellar velocity and velocity dispersion, no correlation is obvious, which makes sense, since attenuation isn’t caused from stars. There’s a different story when comparing the attenuation map to the emission line velocities for $\text{H}\alpha$ and $\text{H}\beta$. Just like the non-star-forming spaxels in the BPT diagram, the spaxels with positive velocities from our view have a medium-correlation with attenuation, and more so with gas that’s moving faster away from us. From this discussion, nothing can be concretely claimed, but inferences can paint the picture. In this non-AGN, young, blue, spiral-like galaxy, there is a haven of star forming activity happening closer to the bulge. There is also a halo of hot, fast moving dust, moving along with similar speed stellar velocities, causing the light from within and po-

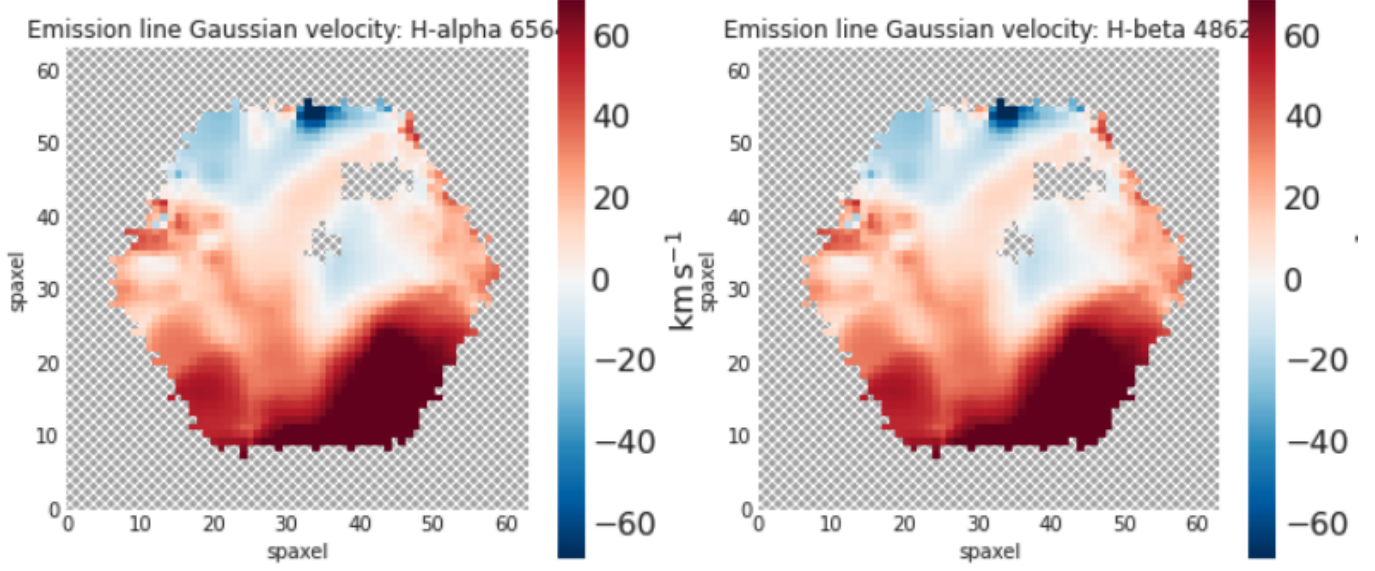


Figure 3. Left: Gas velocity of $H\alpha$. Right: Gas velocity of $H\beta$

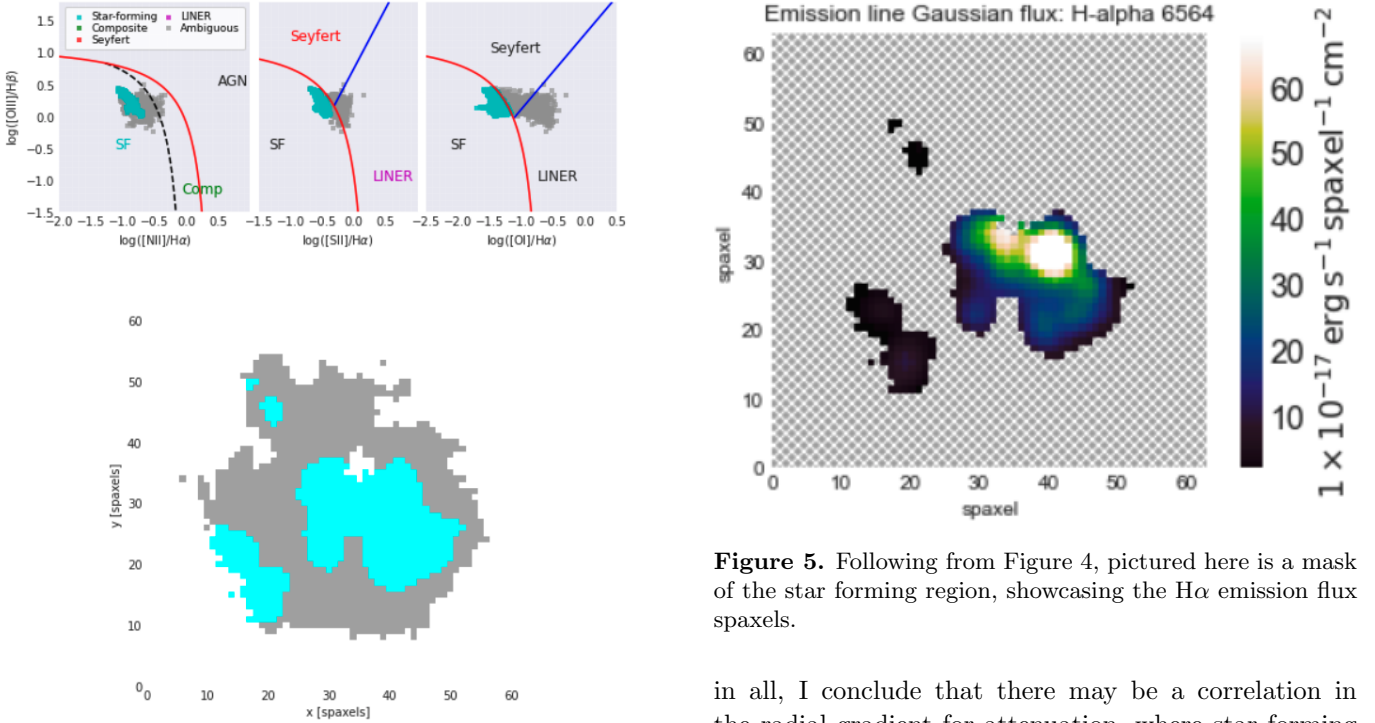


Figure 4. BPT diagram. The blue pixels represent the star forming spaxels, as deduced by the spaxels that fall below the Ka01 classification line (solid red) in each of the 3 diagrams. The Ka03 line represents the H ii-region-like spaxels, and the Ka01 dashed line represents the extreme starburst line. As observed, this galaxy has no active AGN, as the galaxy consists of star forming regions.

tentially even beyond the galaxy to be attenuated. All

Figure 5. Following from Figure 4, pictured here is a mask of the star forming region, showcasing the $H\alpha$ emission flux spaxels.

in all, I conclude that there may be a correlation in the radial gradient for attenuation, where star forming regions and gas velocities may play a role in causing greater attenuation.

4.2. Discussion

One of the main motivations for garnering a deeper understanding for attenuation is to accurately measure galaxy observations while also accounting for the attenuation of light. Galaxy luminosity and SFR is calculated from $H\alpha$ flux emission readings, so it's important to have

accurate readings and account for the attenuation. Such equations are described as:

$$f_{int,H\alpha} = f_{obs,H\alpha} \times 10^{0.4A_{H\alpha}} \quad (3)$$

$$\text{SFR}_{H\alpha}[\text{M}_{\odot}\text{yr}^{-1}] = \frac{L_{H\alpha}[\text{W}]}{2.16 \times 10^{34}\text{M}_{\odot}\text{yr}^{-1}} \quad (4)$$

Where $f_{int,H\alpha}$ is the intrinsic $H\alpha$ flux, $f_{obs,H\alpha}$ is the observed flux, $A_{H\alpha}$ is the $H\alpha$ attenuation, $\text{SFR}_{H\alpha}$ is the $H\alpha$ derived SFR, and $L_{H\alpha}$ is the luminosity of $H\alpha$ (Greener et al. (2020)). As seen, if the intrinsic flux is not account for the amount of attenuation present, the SFR calculation would be off. More research would have to be done to calculate and present exactly how much the attenuation accounts for. The research upon the

stellar and gas kinematics can also be improved as well, as prior research could have also described a support or explanation for a seemingly strong correlation amongst the spacial regions of dust attenuation, gas velocities, and non-star-forming regions.

- 1 We thank Professor Houjun Mo and TA and graduate
- 2 student Alyssa Sokol for teaching and running Astron-
- 3 omy 452H Astrophysics II: Galaxies. We also thank the
- 4 Marvin team, as well as SDSS, for creating a great pro-
- 5 gram and survey that is publicly accessible.

Software: astropy (Astropy Collaboration et al. 2013, 2018), Marvin Cherinka et al. (2019)

REFERENCES

- Astropy Collaboration, Robitaille, T. P., Tollerud, E. J., et al. 2013, A&A, 558, A33, doi: [10.1051/0004-6361/201322068](https://doi.org/10.1051/0004-6361/201322068)
- Astropy Collaboration, Price-Whelan, A. M., Sipőcz, B. M., et al. 2018, AJ, 156, 123, doi: [10.3847/1538-3881/aabc4f](https://doi.org/10.3847/1538-3881/aabc4f)
- Cherinka, B., Andrews, B. H., Sánchez-Gallego, J., et al. 2019, AJ, 158, 74, doi: [10.3847/1538-3881/ab2634](https://doi.org/10.3847/1538-3881/ab2634)
- Domínguez, A., Siana, B., Henry, A. L., et al. 2013, The Astrophysical Journal, 763, 145, doi: [10.1088/0004-637x/763/2/145](https://doi.org/10.1088/0004-637x/763/2/145)
- Greener, M. J., Aragó n-Salamanca, A., Merrifield, M. R., et al. 2020, Monthly Notices of the Royal Astronomical Society, 495, 2305, doi: [10.1093/mnras/staa1300](https://doi.org/10.1093/mnras/staa1300)
- Groves, B., Brinchmann, J., & Walcher, C. J. 2011, Monthly Notices of the Royal Astronomical Society, 419, 1402, doi: [10.1111/j.1365-2966.2011.19796.x](https://doi.org/10.1111/j.1365-2966.2011.19796.x)
- Kewley, L. J., Groves, B., Kauffmann, G., & Heckman, T. 2006, MNRAS, 372, 961, doi: [10.1111/j.1365-2966.2006.10859.x](https://doi.org/10.1111/j.1365-2966.2006.10859.x)